



## **Effects of Lay-Up Sequence and Widths on The SERR of Woven Glass Fiber Reinforced Polymer Composites**

### **Dokuma Cam Elyaf Takviyeli Polimer Kompozitlerin Tabaka Diziliminin ve Genişliklerinin SERR Üzerindeki Etkileri**

**M. Evren Toygar<sup>1</sup>**, **Farshid Khosravi Maleki<sup>2\*</sup>**

<sup>1</sup> Dokuz Eylül University, Engineering Faculty, Mechanical Engineering Department, 35397, İzmir

<sup>2</sup> Bartın University, Engineering Faculty, Mechanical Engineering Department, Bartın

Sorumlu Yazar / Corresponding Author \*: [fmaleki@bartin.edu.tr](mailto:fmaleki@bartin.edu.tr)

Geliş Tarihi / Received: 02.08.2018

DOI:10.21205/deufmd.2019216205

Kabul Tarihi / Accepted: 20.11.2018

Araştırma Makalesi/Research Article

Atıf şekli/ How to cite: TOYGAR, M. E., MALEKİ, F. K. (2019). Effects of Lay-Up Sequence and Widths on The SERR of Woven Glass Fiber Reinforced Polymer Composites. DEUFMD, 21(62), 369-378.

#### **Abstract**

In this paper, fracture behavior of woven Glass Fiber Reinforced Polymer (GFRP) composites under Mode I crack growth was experimentally investigated and numerically modeled, to determine the effects of lay-up sequence and widths on delamination resistance. Different methods are used for calculation of strain energy release rate (SERR): for the experimental solution, experimental compliance calibration method (CCM), modified beam theory (MBT), modified compliance calibration (MCC) are used and virtual crack closure technique (VCCT) are used for the numerical solution. To achieve this aim DCB (double cantilever beam) test specimens are used to evaluate the SERR values. Three-dimensional finite element model is used to perform the delamination, crack analysis, and Mode I SERR value is calculated by the VCCT. It is seen that there is an agreement between experimental and numerical results so that the VCCT method is to be an appropriate method for analyzing a SERR value of woven glass fiber reinforced polymer composites.

**Keywords:** Polymer composites, Fracture toughness, DCB test, Virtual crack closure technique (VCCT)

#### **Öz**

Bu çalışmada, Mod I çatlak ilerlemesi altında dokuma cam elyaf takviyeli polimer (GFRP) kompozitlerinin kırılma davranışı deneysel olarak araştırılmış ve tabaka diziliminin ve numune genişliklerinin delaminasyon direncine olan etkilerini belirlemek için sayısal olarak modellenmiştir. Açığa çıkan şekil değiştirme enerjisinin (SERR) hesaplanması için farklı yöntemler kullanılmıştır: deneysel çözüm için, deneysel uyum kalibrasyon yöntemi (CCM), modifiye edilmiş kiriş teorisi (MBT), modifiye uyum kalibrasyon yöntemi (MCC) kullanılmıştır ve sayısal çözüm için sanal çatlak kapatma tekniği (VCCT) kullanılmıştır. DCB test numuneleri, SERR değerlerini elde etmek için kullanılmıştır. Delaminasyon, çatlak analizi ve Mod I SERR değerlerinin VCCT tarafından hesaplanması için üç boyutlu sonlu eleman modeli kullanılmıştır. Deneysel ve sayısal sonuçların birbiriyle uyumlu olduğu ve böylece bir dokuma cam elyaf takviyeli polimer kompozitlerin SERR değerini analiz etmek için VCCT metodunun uygun bir yöntem olduğu görülmüştür.

**Anahtar Kelimeler:** Polimer kompozitler, kırılma tokluğu, DCB testi, Sanal çatlak kapatma tekniği (VCCT)

## 1. Introduction

Woven fabric reinforced composites are the most important and widely used forms among large transport aircraft structures due to their low density compared to other materials. In recent years, fracture mechanics have found an extensive application in damage analysis of composite laminates, especially in delamination analysis. Delaminations may occur during manufacture because of incomplete curing or may result from impact damage, or they may result from the interlaminar stresses that develop at stress-free edges or discontinuities. Delamination in a composite laminate usually occurs at the interface of differently oriented plies and tends to grow and also it can be a major problem for laminated composite structures [1-5]. The problems of interlaminar performance are discussed along with the technique used to measure them and the fracture mechanics principles applied to improve them. The delamination resistance of laminated composites can be measured by critical SERR (strain energy release rates). The DCB (Double Cantilever Beam) is the most popular specimen configurations in the experimental determination of Mode I interlaminar fracture toughness [6]. Toygar, Toparlı and Uyulgan [7] measured the fracture toughness value of laminated carbon/epoxy composite materials by using the CMOD (crack mouth opening displacement) method experimentally using SENT (Single Edge Notch Tension) specimens. Aliyu and Daniel [8], used conventional double cantilever beam specimens with different configurations to measure the Mode I fracture toughness in a graphite/epoxy composite.

Over the past years, researchers have been investigated the effect of the ply orientations on delamination behavior [9-16]. The effect of stacking sequence on energy release rate distribution across the specimen width the multidirectional DCB specimens is determined by Davidson, Krüger, and König [17]. Effect of the remote ply orientation of DCB laminates with  $\theta//\theta$  and  $\theta//-\theta$  interfaces is investigated by [18,19] and they found that the initiation and propagation values of critical strain energy release rate of 30//30 interface are lower than 30//-30 interface. Schön et al. [20] studied DCB specimens with three different stacking sequences of  $[0]_{24}$ ,  $[(90/0)_2]_s$  and  $[\pm 45/90/0/\pm 45]_{2s}$  and found that the fracture toughness depended on the fiber direction, also the 90//90 interface had the larger propagation energy than

45//45 interface. Nonetheless, considerable research is still required to determine the effect of lay-up sequence and width effects on critical SERR in woven laminated composites.

In this study, the main object is to determine the delamination resistance behavior of plain woven glass fiber reinforced polymer composites. Therefore,  $[0^\circ/90^\circ]_{16}$  and  $[\pm 45^\circ]_{16}$  of plain woven laminated composites with 20, 25, 30, 40 mm width are subjected to Mode I loading to obtain critical SERR. In this way, the compliance calibration method (CCM), modified beam theory (MBT), modified compliance calibration (MCC) have been applied and the recorded load - displacement (F -  $\delta$ ) data are used to quantify the critical SERR of DCB specimen.

3D finite element model has been used for modeling the woven laminated composites to analyze the fracture behavior. The Mode I critical SERR is calculated by the virtual crack closure technique (VCCT). The effect of lay-up sequence and width effects on delamination resistance of woven laminated composites are examined by comparing the three experimental method and numerical results.

## 2. Material and Method

In this study, plain woven fabric-reinforced glass/epoxy composite laminates were fabricated with two different orientation configurations,  $[0^\circ/90^\circ]_{16}$  and  $[\pm 45^\circ]_{16}$  by hand layup at the composite laboratory of Mechanical Engineering Department, Dokuz Eylül University. It has sixteen plies of glass plain weave fabric (0.85 kg/m<sup>2</sup>) of approximately 60% volume fraction as the reinforcement and epoxy resin was used to produce GFRP (Glass Fiber Reinforced Polymer) plate. A thin non-adhesive Teflon film with 0.07 mm thickness was placed at the mid-plane (between 8th and 9th plies) to simulate an initial delamination by considering ASTM Standard D5528-13 [21] as seen in Figure 1.

### 2.1 Specimen preparation for mechanical testing

Tensile and shear properties of the composite were measured by ASTM D3039/3039M-17 [22] ASTM D3518/D3518M-13 [23], respectively. Specimens were prepared according to the ASTM suggestion as seen in Figure 2.

The obtained mechanical properties of woven-fabric-reinforced glass/epoxy composite by using video extensometer are given in Table 1.

**Table 1.** Physical and mechanical properties of plain woven fabric-reinforced glass/epoxy composite laminates.

Lay-up sequence	Poisson ratio ( $\nu$ )		Modulus of elasticity (GPa)			Shear Modulus (GPa)
	$\nu_{12}$	$\nu_{13}$	$E_{11}$	$E_{22}$	$E_{33}$	$G_{12}$
$[0^\circ/90^\circ]_{16}$	0.28	0.3	28	28	15	4.7
$[\pm 45^\circ]_{16}$	0.35	0.4	12	12	8	6

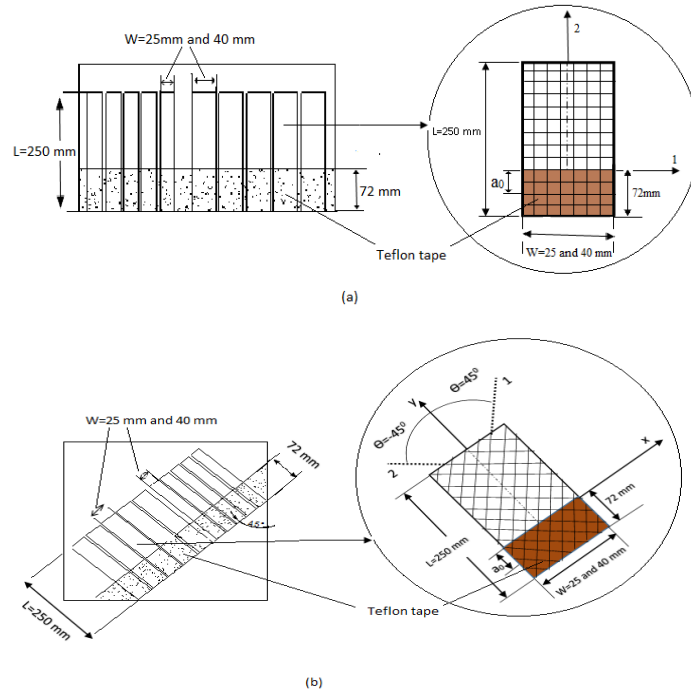


**Figure 1.** The detail of the cutting of sample from the manufactured woven-GFRP composite plate a) ( $0^\circ/90^\circ$ ) fiber orientation, b) ( $\pm 45^\circ$ ) Fiber orientation.

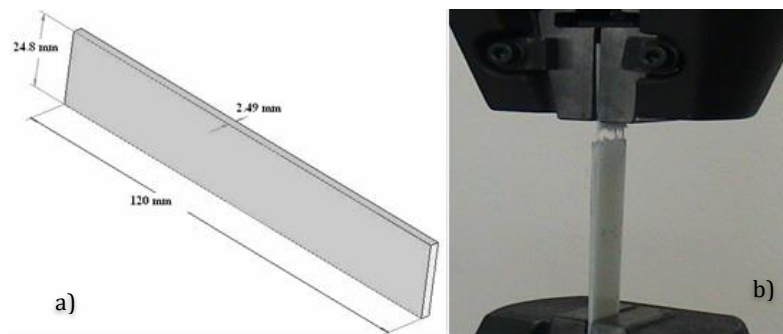


**Figure 2.** a) Geometries of the test specimen for mechanical properties testing, b) view of tension test

**2.2 Specimen preparation for fracture testing**

DCB specimens for fracture testing were prepared with dimensions of  $W = 20$  mm, 25 mm, 30 mm and 40 mm specimen width,  $L = 250$  mm total length,  $h = 2,5$  mm the thickness, and  $a_0 = 47$  mm initial crack length according to ASTM Standard D5528-13 as shown in Figure 3.

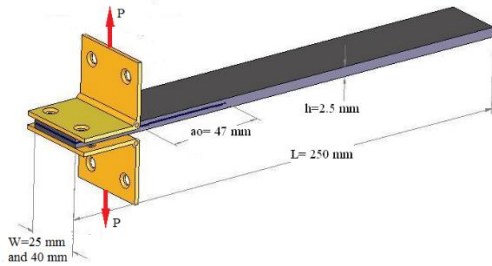


**Figure 3.** The dimensions of DCB test specimens.

**2.3 Fracture testing and data reduction**

Tests were performed in a universal testing machine (Shimadzu AG-100) under displacement control with a crosshead rate of 2 mm/min. The hinges were bonded on the specimen with epoxy adhesive and tensile loads were applied to the specimen via pins through universal joints (See Figure 4). The specimens were aligned and centered with the help of a level while mounting the hinges on the load grips. Crack propagation was monitored with the help of video extensometer. For the measurement of crack growth, marks were indicated every 1 mm from the crack tip, then marks were applied every 5 mm. For the DCB test specimen, the recommended extent of crack propagation is 65 mm. The tests were performed at constant room conditions of 22°C and relative humidity was 50%.



**Figure 4.** Experimental Setup for DCB Test.

The characteristic load-displacement curves of woven  $[0^\circ/90^\circ]_{16}$  and  $[\pm 45^\circ]_{16}$  specimens with different specimen widths were obtained. The initiation and propagation values of critical strain energy release rate  $G_{IC}$  can be derived from the recorded load-displacement data. The mean characteristic load-displacement behavior for some samples has been given in Figure 5. Initiation of delamination is determined by a deviation from linearity.  $G_{IC}$  can be calculated using the load and displacement at the point of non-linearity of the load-displacement curve. The unloading curve was also registered, as in case of significant permanent deformations and/or non-linearity. The camera was positioned at a distance 1000 mm away from the

specimen surface. Images are captured during the test using two CCD-cameras to get crack mouth opening displacement (CMOD).

To observe the delamination (crack) growth and to identify crack extension  $\Delta a$  in mm during the loading, visual observation has been done and the gripped hinges were pulled apart with a crosshead speed of 2 mm/min in displacement control until satisfactory crack growth occurred in the specimen. First, the loading was continued with a crosshead speed of 2 mm/min up to the displacement of about 28 mm and crack propagation  $\Delta a$  2-3 mm occurs. Then the crosshead was returned to zero point with 25 mm/min constant displacement speed to form a natural pre-crack. Second, the loading was

continued with a crosshead speed of 2 mm/min up to the displacement of about 65 mm, after then the crosshead was returned to zero displacement with 25 mm/min constant displacement speed.

**2.3.1 Compliance calibration method (CCM)**

The method of data reduction is explained as reported in ASTM Standards as follow:

CCM is used to determine the critical SERR,  $G_{IC}$ . Therefore,  $G_{IC}$  is:

$$G_{IC} = \frac{nP_c \delta}{2W a} \tag{1}$$

where;  $P_c$  is the critical load,  $a$  is crack length,  $W$  is the specimen width,  $\delta$  is load point

displacement in mm (Figure 5). CCM generates a least squares plot of  $\log(\delta_i/P_i)$  as compliance versus  $\log(a_i)$  as seen in Figure 6, where  $i$  represents the number of specimen and changes from 1 to 5, to use the visually observed delamination onset values and all the propagation values. The slope of this line is  $n$ .

The average  $G_{IC}$  value of  $[0^\circ/90^\circ]$  and  $[\pm 45^\circ]$  fiber orientation specimens for different widths with error bars are obtained and given in Figure 7. As it is seen from the figure, the energy release rate decreases with increasing specimen width for different fiber orientation.

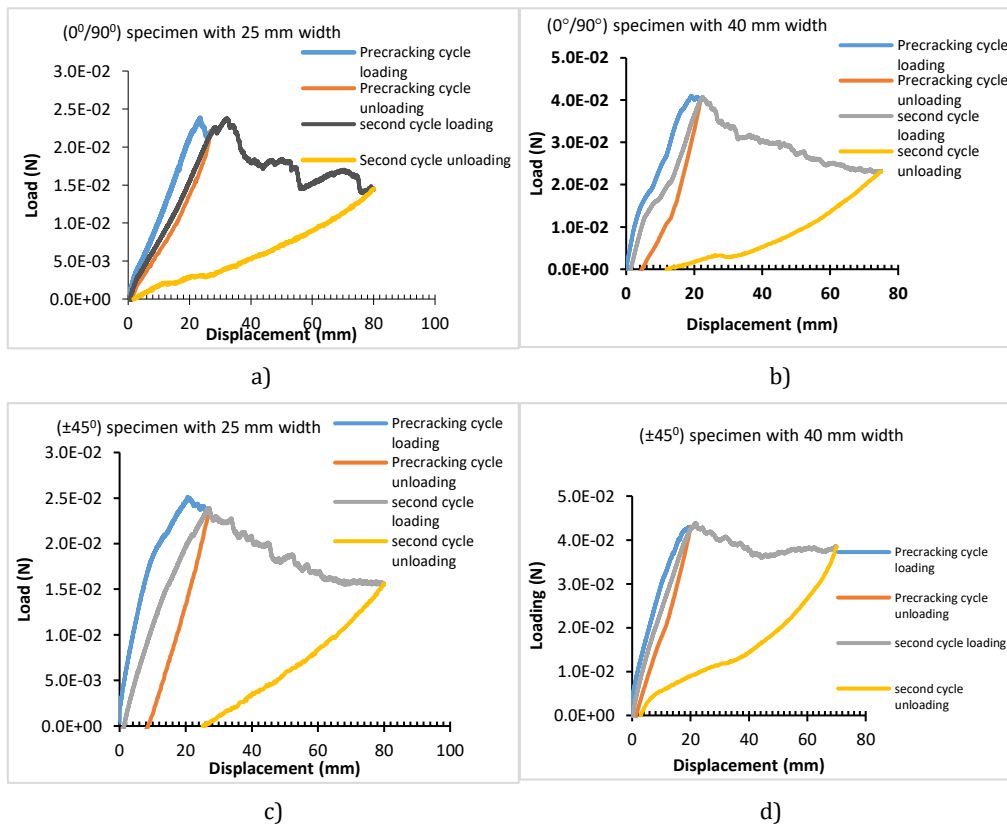


**Figure 5.** Load-displacement characteristics for some samples, a) woven  $[0^\circ/90^\circ]_{16}$  with 25 mm width, b) woven  $[0^\circ/90^\circ]_{16}$  with 40 mm width, c) woven  $[\pm 45^\circ]_{16}$  with 25 mm width, d) woven  $[\pm 45^\circ]_{16}$  with 40 mm width

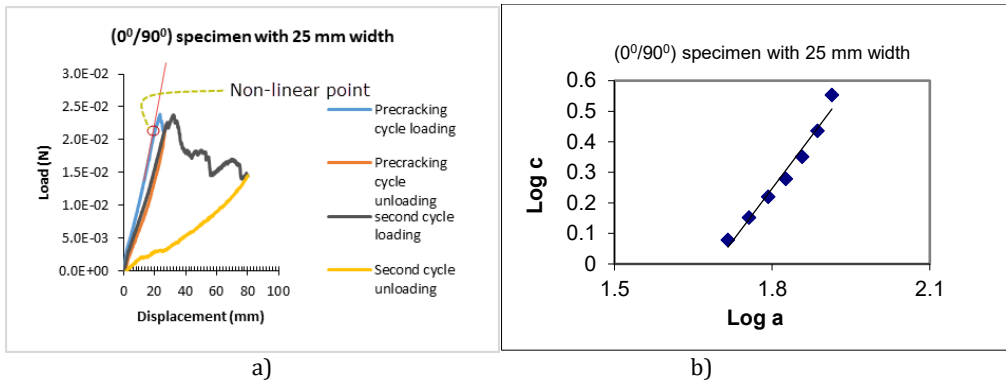


Figure 6. a) Load-displacement characteristics. b) Log ( $\delta/P$ ) as compliance versus log (a) for Sample 4.

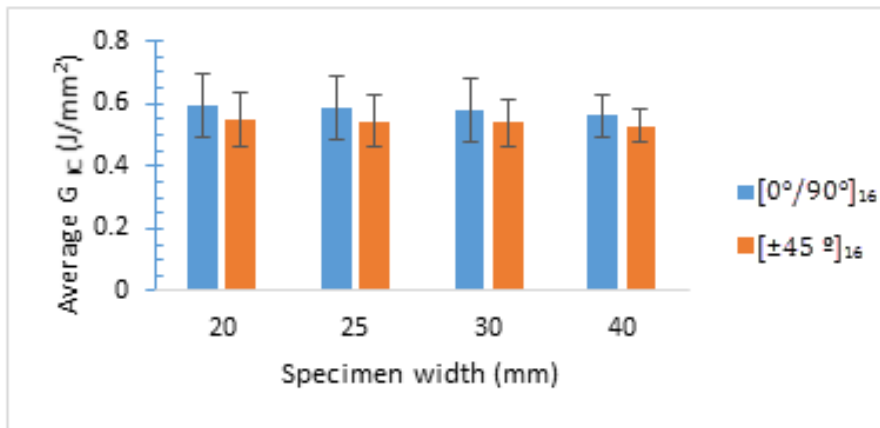


Figure 7. Influence of width on average  $G_{IC}$  of CCM for  $[0^\circ/90^\circ]$  and  $[\pm 45^\circ]$  woven laminates. Error bars are  $\pm 1$  standard deviations.

### 2.3.2 Modified beam theory (MBT) method

As reported in ASTM Standard, the critical SERR,  $G_{IC}$  by using MBT can be calculated by

$$G_{IC} = \frac{3P\delta}{2b(a + |\Delta|)} \quad (2)$$

where;  $P$  is the critical load,  $a$  is crack length,  $b$  is the specimen width,  $\delta$  is load point displacement in mm.  $\Delta$  may be determined experimentally by generating a least squares plot of the cube root of compliance,  $C^{1/3}$ , as a function of delamination length. The compliance,  $C$ , is the ratio of the load point displacement to the applied load,  $\delta/P$  (Figure 8).

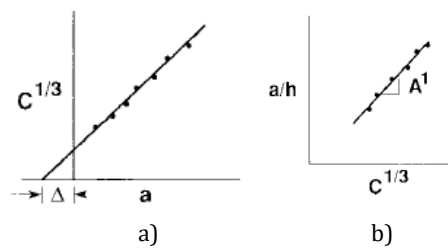


Figure 8. a) Modified Beam Theory, b) Modified Compliance Calibration [10].

**2.3.3 MCC (Modified compliance calibration) method**

The method of data reduction is explained as reported in the ASTM Standard. MCC is used to determine the critical SERR,  $G_{Ic}$ . Therefore,

$$G_{Ic} = \frac{3P^2C^{2/3}}{2A^1bh} \tag{3}$$

where;  $P$  is the critical load,  $b$  is the specimen width,  $h$  is the specimen thickness. Generate a least squares plot of the delamination length normalized by specimen thickness,  $a/h$ , as a function of the cube root of compliance,  $C^{1/3}$ . The compliance,  $C$ , is the ratio of the load point displacement to the applied load,  $\delta/P$ . The slope of this line is  $A^1$  (Figure 8).

**2.4. Numerical analysis**

The virtual crack closure technique (VCCT) is widely used for computing energy release rates, based on results from continuum (2D) and solid (3D) finite element (FE) analyses. VCCT was first proposed by Rybicki and Kanninen [24] based on the principles of Linear elastic fracture mechanics(LEFM). It is an effective method in solving delamination problems and used in modeling delamination growth in composites [25]. Krueger [26] covers the technique and its applications extensively.

VCCT is based on the assumption that the strain energy released in the crack propagation process is equal to the energy required to close the crack to its original state. The advantage of VCCT is its numerical simplicity and effectiveness. The calculation of Mode I strain energy release rate  $G_I$  for each eight-node element position along the delamination front can be summarized by the following equation [27]:

$$G_I = -\frac{1}{2\Delta A} R_y \Delta V \tag{4}$$

Where  $G_I$  is Mode I energy release rate,  $\Delta A$  is the crack extension area;  $R_y$  is the vertical force at the crack tip,  $\Delta V$  is the vertical displacements between the top and bottom nodes of the crack face in y direction, respectively (Figure 9).

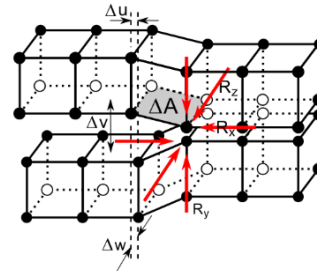


**Figure 9.** VCCT for eight-node solid element [27].

Mode I delamination was simulated using the Ansys 15 (Figure 10). 3D finite element model (SOLID185, eight-node element) has been used for modeling of the structure. Delamination is modeled as a discrete discontinuity in the center of the DCB specimen with separate unconnected nodes on the upper and lower surfaces of the delamination section. The model is divided into 100 elements in length, 21 elements in width, and 4 elements in thickness. The critical SERR has been calculated using the virtual crack closure technique (VCCT). Material properties used are shown in Table 1. All dimensions and boundary conditions are similar to the real experimental set-up, in order to provide acceptable comparisons (Figure 10). In this section, the loads corresponding to the point of non-linearity of the load-displacement curve in the DCB specimen were used to calculate the critical strain energy release rates, using nonlinear elastic finite element models and Ansys implementation of VCCT.

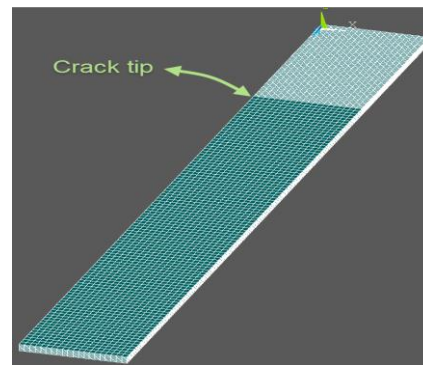


**Figure 10.** Finite element model of the DCB specimen.

**3. Results**

The woven GFRP composites with  $[0^\circ/90^\circ]_{16}$  and  $[\pm 45^\circ]_{16}$  stacking sequence have been studied

and the mechanical properties and interlaminar toughness,  $G_{IC}$  value are obtained experimentally and numerically. Figure 5 shows a typical load-displacement curve for some samples of woven  $[0^\circ/90^\circ]_{16}$  and  $[\pm 45^\circ]_{16}$  specimens. It is seen that some degree of non-linearity and small permanent deformations are visible in the unloading curves of specimens. The non-linearity can be partly attributed to the

specimens undergoing relatively large displacements towards the end of the tests.

The critical SERR,  $G_{IC}$  can be calculated from the recorded load-displacement data by using CCM, MBT and MCC methods. The effect of width on average  $G_{IC}$  for  $[0^\circ/90^\circ]$  and  $[\pm 45^\circ]$  fiber orientation specimens are given in Table 2. It is seen that  $[0^\circ/90^\circ]$  stacking sequence specimens have higher toughness values than,  $[\pm 45^\circ]_{16}$ .

**Table 2.** The interlaminar toughness of the woven GFRP with different lay-up sequence and width.

lay-up sequences and widths of specimens		$[0^\circ/90^\circ]_{16}$				$[\pm 45^\circ]_{16}$			
		20	25	30	40	20	25	30	40
$G_{IC}$ (J/mm <sup>2</sup> )	CCM	0.59	0.58	0.57	0.56	0.54	0.54	0.53	0.53
	MBT	0.69	0.69	0.68	0.68	0.66	0.66	0.66	0.65
	MCC	0.61	0.61	0.60	0.60	0.59	0.59	0.59	0.59
	VCCT	0.62	0.62	0.61	0.59	0.57	0.56	0.56	0.55

According to obtained results given in table 2, CCM and MCC methods have close results and MBT results deviate from CCM and MCC results. As it is seen from Table 2, in experimental results, the characteristic behavior of toughness is the same. It means that critical SERR decreases slightly relative to the amount of increasing width. For example, in CCM results when the specimen width increases from 20 mm to 40 mm, the toughness value decreases 5.05% and 3.28% for woven  $[0^\circ/90^\circ]_{16}$  and  $[\pm 45^\circ]_{16}$ , respectively. Nevertheless, the energy release rate decreases slightly with increasing specimen width for both types of woven specimens. Furthermore, the obtained experimental toughness value of woven  $[0^\circ/90^\circ]_{16}$  specimen is greater averagely 6.77% than woven  $[\pm 45^\circ]_{16}$  specimen. In the 0//90 interface, the matrix cracking occurs during the delamination propagation which absorbs extra energy. Shokrieh et al. [16] found that the initiation and propagation of fracture toughness of the E-glass/epoxy DCB specimen with 0//0 interface is less than other specimens and by changing the direction of fibers at the interface, e.g., 0//30, 0//45 and 0//90, more energy is needed to peel off fibers from the fracture surface.

Finite element analysis was conducted to validate the closed form solution. By using VCCT, the toughness value  $G_{IC}$  has been obtained for DCB specimens numerically. As it is seen from Table 2, VCCT results show good agreement with

CCM and MCC results. for example,  $[0^\circ/90^\circ]_{16}$  specimens the differences between numerical and CCM results are approximately 5.57% for 20 mm width, 3.2% for 25 mm width, 5.7% for 30 mm width and 6.01% for 40 mm width. For  $[\pm 45^\circ]_{16}$  specimens the differences between numerical and CCM are approximately 4.19% for 20 mm width, 3.88% for 25 mm width, 3.75% for 30 mm width and 4.5% for 40 mm width. As a result of numerical analyses, it can be seen that the toughness decreases slightly relative to the amount of increasing width, it means that the change of width of DCB specimen is not a great effective parameter for interlaminar toughness values.

The results of the experimental test and numerical analysis showed good agreement demonstrating the effectiveness of the proposed experiment and numerical methods lamination through the thickness.

#### 4. Discussion and Conclusion

The problems of interlaminar performance are discussed along with the technique used to measure them and the fracture mechanics principles applied to improve them. In this study, to research and verify the compatibility of experimental and numerical studies CCM, MBT and MCC methods are applied to the laminated composites to observe fracture characteristics and the effect of width and stacking sequence with different orientations of woven GFRP on

fracture parameters. It has been obtained that woven  $[0/90]_{16}$  specimens have higher toughness values than woven  $[\pm 45^\circ]_{16}$  specimens. Some decreases have been eventuated in toughness values by an increase in width.

As mentioned in ASTM D5528-13 standards for unidirectional laminates, the change of width of DCB specimen is not an effective parameter for interlaminar toughness values and in this paper, it is seen that width parameter is not very effective on interlaminar toughness value on woven GFRP also. It is concluded that the SERR

value of DCB specimens of woven GFRP is independent of the specimen width.

VCCT for crack growth analyses of woven GFRP has been studied. It is seen that the obtained energy release rate values in CCM and MCC were close to the value  $G_{Ic}$  found in VCCT analysis and MCC gives the best agreement with VCCT. It is concluded that VCCT analysis is to be an appropriate method for analyzing a strain energy release rate of woven GFRP. Also, the average SERR values showed only small variations with different stacking sequence due to the orientation of fiber angle.

## References

- [1] Hyer M.W.: Stress analysis of fiber-reinforced composite materials. McGraw-Hill, Massachusetts, (1998).
- [2] Broek D.: Elementary Engineering Fracture Mechanics. Kluwer Academic Publishers, Boston, Massachusetts, (1996).
- [3] O'Brien T.K.: Fracture Mechanics of Composite Delamination. Composites: ASM International, 21, 241-245 (2001).
- [4] O'Brien, T. K.: Characterization of delamination onset and growth in a composite laminate. Damage in composite materials, ASTM STP 775/2, 140-167 (1982).
- [5] Tay T. E.: Characterization and analysis of delamination fracture in composites: an overview of developments from 1990 to 2001, Applied Mechanics Reviews 56/1, 1-32 (2003). DOI:10.1115/1.1504848
- [6] De Morais A.B., De Moura M.F., Marques A.T., De Castro P.T.: Mode-I interlaminar fracture of carbon/epoxy cross-ply composites. Composites Science and Technology, 62/5, 679-686 (2002). DOI:10.1016/S0266-3538(01)00223-8
- [7] Toygar M.E., Toparli M., Uyulgan B.: An investigation of fracture toughness of carbon/epoxy composites. Journal of reinforced plastics and composites, 25.18, 1887-1895 (2006). DOI: 10.1177/0731684406069916
- [8] Aliyu A.A., Daniel I.M.: Effects of strain rate on delamination fracture toughness of graphite/epoxy. Delamination and debonding of materials, ASTM STP, 876, 336-348 (1985).
- [9] Chai H.: The characterization of Mode I delamination failure in non-woven, multidirectional laminates. Composites, 15, 277-90 (1984).
- [10] Choi NS, Kinloch AJ, Williams JG.: Delamination fracture of multidirectional carbon-fiber/epoxy composites under Mode I, Mode II and mixed-Mode I/II Loading. J Compos Mater, 33, 73-100 (1999).
- [11] Canturri C, Greenhalgh ES, Pinho ST, Ankersen J.: Delamination growth directionality and the subsequent migration processes – the key to damage tolerant design. Compos Part A Appl Sci Manuf, 54, 79-87 (2013).
- [12] Pelegri AA, Tekkam A.: Optimization of laminates' fracture toughness using design of experiments and response surface. J Compos Mater, 37, 579-96 (2003).
- [13] Pereira AB, de Morais AB.: Mode I interlaminar fracture of carbon/epoxy multidirectional laminates. Compos Sci Technol, 64, 2261-70 (2004).
- [14] Sebaey TA, Blanco N, Costa J, Lopes CS.: Characterization of crack propagation in mode I delamination of multidirectional CFRP laminates. Compos Sci Technol, 72, 1251-6 (2012).
- [15] Chou I, Kimpara I, Kageyama K, Ohsawa I.: Mode I and Mode II Fracture Toughness Measured Between Differently Oriented Plies in Graphite/Epoxy Composites. Compos Mater Fatigue Fract – Fifth Vol ASTM STP 1230, Martin RH, editor. Am Soc Test Mater Philadelphia, 132-51 (1995).
- [16] Shokrieh MM, Heidari-Rarani M.: Effect of stacking sequence on R-curve behavior of glass/epoxy DCB laminates with 0//0 crack interface. Mater Sci Eng, A, 529, 265-9 (2011).
- [17] Davidson B.D., Krüger R., König M.: Effect of stacking sequence on energy release rate distributions in multidirectional DCB and ENF specimens. Engineering Fracture Mechanics, 55/4, 557-569 (1996).
- [18] Hudson R.C., Davidson B.D., Polaha J.J.: Effect of remote ply orientation on the perceived mode I and mode II toughness of h/h and h/h interfaces, Appl. Compos. Mater. 5, 123-138 (1998).
- [19] Polaha J.J., Davidson B.D., Hudson R.C., A.: Pieracci, Effects of mode ratio, ply orientation and precracking on the delamination toughness of a laminated composite, J. Reinf. Plast. Compos. 15, 141-173 (1996).
- [20] Schön J., Nyman T., Blom A., Ansell H.: A numerical and experimental investigation of delamination behaviour in the DCB specimen, Compos. Sci. Technol. 60, 173-184 (2000).
- [21] ASTM D 5528-13.: Standard test method for mod 1 interlaminar fracture toughness of unidirectional fiber-reinforced polymer matrix composites. ASTM Annuo of Standards, West Conshohocken, PA, USA, 2013.
- [22] ASTM D3039 / D3039M-17, Standard test method for tensile properties of polymer matrix composite materials, ASTM International, West Conshohocken, PA, USA, 2017.

[23] ASTM D3518-D3518M-13.: Standard test method for in-plane shear response of polymer matrix composite materials by tensile test of a  $\pm 45$  degree Laminate. ASTM Annual Book of Standards, West Conshohocken, PA, USA, 2001.

[24] Rybicki E.F., Kanninen M.F.: Finite element calculation of stress intensity factors by a modified crack closure integral, *Engineering Fracture Mechanics*. 9, 931-938 (1977). DOI:10.1016/0013-7944(77)90013-3

[25] Shen F., Lee K.H., Tay, T.E.: Modeling delamination growth in laminated composites. *Composites Science and Technology*, 61(9), 1239-1251 (2001).

[26] Krueger R.: Virtual crack closure technique: history, approach and applications. *Applied Mechanics Reviews*, 57 (2), 109-143 (2004). DOI:10.1115/1.1595677

[27] Research, A.A.: Release 15.0, Help System. In. ANSYS Structural Analysis Guide. ANSYS, Inc, (2015)